Bio-phenolic compounds production through fast pyrolysis: demineralizing olive pomace pretreatments

A. Alcazar-Ruiz, F. Dorado, L. Sanchez- Silva*

Department of Chemical Engineering, University of Castilla –La Mancha,

Avda. Camilo José Cela 12, 13071 Ciudad Real, Spain

*e-mail: *marialuz.sanchez@uclm.es*

Abstract

An original pathway to renewable production of phenol-rich bio-oil by fast pyrolysis of pretreated olive pomace (OP) was researched. However, inherent inorganic elements (especially alkali and alkaline earth metals) in biomass feedstocks largely modified the final bio-oil composition. To alter their catalytic activity in fast pyrolysis, different demineralisation processes (water, acid and alkali pretreatments) were employed. There was also an in-depth study of bio-oil phenolic compounds, analysing the oxygen-containing substituted groups linked to the benzene ring. From water leached samples, potassium was largely removed, enhancing the selective production of guaiacol (at room temperature) and syringol (at T = 90 ºC). Important differences were observed with HCl and HNO_3 pretreatments regarding carboxylic acid and phenolic distribution. For pretreatment with NaOH, the sodium content in the sample was observed to increase to 83%. Thus, optimal phenolic selectivity (36.9%) was achieved for the alkali pretreated OP sample, where guaiacol (5.9%) and vinyl guaiacol (6.2%) yields increased and methyl guaiacol decreased. This study marks an efficient and clean pathway for converting agricultural waste into valuable phenolic enriched bio-oil. This could constitute a new way of obtaining these compounds by using renewable agriculture biomass.

Keywords: olive pomace, fast pyrolysis, demineralization pretreatment, renewable phenolics, guaiacol, syringol.

1. Introduction

Phenolic compounds have a wide range of applications in production areas such as food additives, energy, fine chemicals, and phenolic resins (Schmidt, 2005). Moreover, phenol production has grown at an average rate of 1.8 % per year, but still does not meet demand due to the ever increasing rate of consumption (Duan et al., 2019). Most industrially produced phenols comes from benzene in a three-step cumene process. This entails consuming great amounts of fossil fuels and damages the environment (Zhang et al., 2018). In this paper, lignocellulosic biomass is set out as a renewable alternative pathway for producing these types of compounds. Biomass has attracted interest as it is sustainable and universally carbon-neutral and is a precursor for producing bio-chemicals. Thermochemical processes are one of the main technologies for using biomass, in which pyrolysis is a promising and effective method for converting it into energy and chemicals (Zhang et al., 2022). Specifically, fast pyrolysis is known to convert lignocellulosic biomass into high energy storage forms to be used as an energy carrier, such as bio-oil (Hu and Gholizadeh, 2019). However, there has been relatively little research into promising applications of olive pomace feedstock. Olive pomace is one of the main subproducts obtained from olive oil extraction, which is an important economic sector in Mediterranean countries. Its composition depends on the olive variety, soil, environmental conditions and the processing method. Olive pomace is typically known for containing water-soluble fats, proteins, water-soluble carbohydrates and water-soluble phenolic substances (Dorado et al., 2020; Ducom et al., 2020). Some of its features are its high moisture content, slightly acidic pH values and high amount of organic matter, particularly lignin (Miranda et al., 2019). Lignin is a three-dimensional phenylpropanoid unit containing a polymer, embedded within a cellulose and hemicellulose matrix in the plant cell walls (Kumar et al., 2021). It is the most abundant aromatic biopolymer in

nature, which accounts for 15-30 wt.% and 40% of the energy from lignocellulosic biomass (X. Chen et al., 2019a). Therefore, phenol can be obtained by lignin degradation providing a new pathway for clean phenol production from renewable feedstocks. The main components obtained in bio-oil from fast pyrolysis of lignin are oxygenated phenolics, presented as hydroxyl (–OH), methoxyl ($–OCH_3$), and the aryl ether bond (β–O–4 and α–O–4), accounting for 70% of total bio-oil components (Huang et al., 2020a).

Biomass pretreatment prior to fast pyrolysis has proved to be a cost-effective method for upgrading bio-oils. In relation to this, alkali and alkaline earth metals (AAEMs) inherent in biomass have a significant impact on bio-oil fast pyrolysis product distribution (Zhang et al., 2022). Generally, AAEMs are mainly composed of water-soluble alkali metals (NaCl, KCl, Na_2CO_3, K_2CO_3, etc.), ion-exchange alkali metals associated with an organic matrix, and acid-soluble alkali metals (mainly alkaline earth metals) (Y. Chen et al., 2020; Mlonka-Mędrala et al., 2020). AAEMs species could lower the quality of bio-oil by promoting the formation of water and organic acids (Niu et al., 2022). Therefore, cost-effective demineralization processes should be developed to remove these minerals from olive pomace and thus enhance production of phenolic compounds. Pretreatment techniques have been further studied to remove AAEMs, like water, acid and alkali leaching (Persson and Yang, 2019). In a previous work it was suggested that water leaching is highly effective at demineralization in terms of removing alkali metalloids (largely potassium with a demineralization efficiency of 91%) from an olive pomace feed (Alcazar-Ruiz et al., 2021). In contrast, acid washing could effectively remove AAEMs from biomass resulting in fewer catalytic reactions and less pyrolytic slagging (Li et al., 2022). Acid pretreatment could accelerate the demethoxylation and cleavage of aryl ether linkages in the biomass structure, and further enhance the result of phenol yields in bio-oil from fast pyrolysis (Duan et al., 2019). In this respect, Ma et al. reported that HCl

pretreatment of lignin enhanced depolymerisation of the lignin matrix, which led to an increase in the liquid yield (42.5 wt.%) corresponding to the phenol fraction (Ma et al., 2017). In addition, alkali washing is known to be an effective pretreatment method for changing the fiber structure and composition by solubilisation of cellulose and lignin (Li et al., 2022). Dalle et al. (2021) studied sodium hydroxide (NaOH) pretreatment to remove amorphous compounds from lignin, hemicellulose and extracts, thus increasing thermal stability. Additionally, a great deal of previous research mainly focused on the performance of lignin subjected to pyrolysis for producing high-purity phenols. Duan et al. (2021) reported that acid pretreatment of lignin accelerated degradation of the lignin matrix (Duan et al., 2021). To the best of our knowledge, there has been very little research on using agricultural waste biomass, such as olive pomace (known for being high in water-soluble phenolic substances) for obtaining renewable bio-phenolics. Moreover, demineralization techniques for selective phenolic compounds via fast pyrolysis of olive has not been studied. Therefore, removing AAEMs before subjecting olive pomace to fast pyrolysis is the main influencing factor in the production of phenolic compounds which must be considered.

Herein, the influence of demineralization pretreatment by different solvents was further researched for selective phenolic yields of olive pomace feedstock via fast pyrolysis. In this paper, water at room temperature (25 ± 3 ºC) and at 90 ºC, three different hydrochloric acid solvent concentrations, nitric acid and sodium hydroxide were used to pretreat olive pomace which were then fast pyrolysed to enhance bio-oil production. This study concerns finding a clean and efficient way of creating renewable phenolic compounds using a cost-effective thermochemical technique such as fast pyrolysis. Furthermore, the use of pretreated olive pomace could provide a new strategy for valorising the use of environmentally friendly agro-industrial residues.

2. Material and methods

2.1. Materials

Olive pomace (OP) used in this work was provided by an olive oil mill from the region of Castilla- La Mancha (Spain). This OP comes from an olive harvest of the cornicabra variety. A detailed description of the material received from the mill is given elsewhere (Parascanu et al., 2018; Puig-Gamero et al., 2021). The biomass sample was oven-dried for 24 h at 100 ºC, and then ground and sieved to obtain an average particle size ranging from 100 to 150 µm using a mill type 2 sharp blades blender (GRINDOMIX GM 200, Retsch). High-purity hydrochloric acid (ACS reagent, 37%), nitric acid (ACS reagent, 70%), and sodium hydroxide (ACS reagent ≥ 97%, pellets) were purchased from Sigma-Aldrich (Saint Louis, MO, USA).

2.2. Demineralization process

OP was leached with four different agents for removing inorganics: deionized water, hydrochloric acid (HCl), nitric acid (HNO_3) and sodium hydroxide (NaOH). In the water leaching technique, the samples (1 g of solid per 20 ml of deionized water) were shaken at room temperature (25 ± 3 ºC) and at 90 ºC with a magnetic stirrer for 2 h and then vacuum filtered (filter paper 110mm, pore retention 25 µm, ash content <0.1%). Then, samples named as OP-H_2OT25 and OP-H_2OT90 refer to the OP sample after demineralization by deionized water leaching at room temperature and at 90 ºC, respectively. For the acid leaching, the total volume of liquid was 20 ml per gram of OP, following a procedure described in literature (Jiang et al., 2013a). As for HCl leaching, this acid was diluted to 2.5%, 5% and 10 wt.% solutions which were used to prepare OP-2.5HCl, OP-5HCl and OP-10HCl, respectively. To compare the effects of acid, HNO_3 was prepared at a concentration of 10 wt.%. The corresponding sample was denoted as OP-HNO_3. In order to know what effect alkali leaching had, NaOH at 10 wt.% was

selected to demineralize OP and the resulting sample was denoted as OP-NaOH. All procedures were immersed in their respective prepared solutions and stirred magnetically for 2 h at room temperature (25 ± 3 ºC). The biomass sample was recovered by filtration and washed with Milli-Q water until the pH value was neutral. After rinsing, all biomass samples were oven-dried at 105 ºC for 24 h.

2.3. Samples characterization

Firstly, raw and demineralized samples were characterized by elemental and thermogravimetric analysis using a TGA apparatus (TGA 2, Mettler Toledo). Proximate and ultimate analyses were carried out to determine what compositions the different samples had (following standards UNE 15104:2011, UNE-EN ISO18123, UNE 32-004-84 and UNE 32-002-95) in the elemental analyser Flash Smart Elemental Analyser (Thermo Scientific) equipped with a thermal conductivity detector. The proximate analysis yielded information on volatile matter, fixed carbon and ash content. The ultimate analysis was used to find the concentration of carbon, hydrogen, nitrogen, oxygen and sulphur in the sample. The higher heating value (HHV) could be calculated using the ultimate analysis data with the following empirical correlation (Eq. 1 (A. Alcazar-Ruiz et al., 2021); Table 1):

$$HHV\left(\frac{MJ}{kg}\right) = 0.3491 \cdot C + 1.1783 \cdot H + 0.1005 \cdot S - 0.1034 \cdot O - 0.0151 \cdot N - 0.0211 \cdot A \quad [1]$$

In which *C*, *H*, *S*, *O* and *N* are the weight percentages for carbon, hydrogen, sulphur, oxygen and nitrogen respectively, whereas *A* is the weight percentage for ash.

The alkali and alkaline earth metals (AAEMs) content in each sample was determined by Inductively Coupled Plasma-Optical Emission Spectrometry (ICP-OES). Here, Varian

720-ES equipment (which was previously calibrated using standard stock solutions) was used and whose results are listed in Table 2. The chemical composition of OP was tested according to the TAPPI 204 om-97 and TAPPI T222 om-02 methods and following Miranda et al., (2019) and (TAPPI, 2018) to obtain the ratios of extractives, hemicellulose and Klason lignin whose results are given in Table 1.

Fourier Transform Infrared Spectroscopy (FTIR) was used to identify potential chemical structural differences after demineralization. The IR spectra was performed with a Perkin-Elmer FTIR Spectrum-two spectrophotometer equipped with a Universal Attenuated Total Reflectance Accessory (UATR). The spectra accumulated 64 scans with a wavenumber range between 500 and 4000 cm^{-1} and a resolution of 8 cm^{-1}.

2.4. Fast pyrolysis procedure analysis

The fast pyrolysis experiments on raw and demineralised samples were carried out using a Pyroprobe 6200 pyrolysis (CDS analytical) connected to a 7890B/5977B GC/MS analyser (Agilent Technologies) with a transfer line (length: 1 m; temperature: 340 ºC).

The GC/MS injector temperature was maintained at 280 ºC. An Elite-35MS capillary column (30 m x 0.25 µm) was used for chromatographic separation. Helium (99.999 %) was selected as the carrier gas at a constant flow rate of 1 ml/min and a 1:80 split ratio. The purpose of this was to separate the different chemicals in the bio-oil and to identify them. The oven temperature was programmed from 40 ºC (3 min) to 280 ºC at a heating rate of 5 ºC/min. The chromatograms were integrated, and the relative peak areas were calculated and, subsequently identified using the National Institute of Standards & Technology (NIST) library as a reference ("Libro del Web de Química del NIST," n.d.). Only peaks with a matching quality of over 80% were considered.

Raw and demineralised OP samples (1 mg ± 0.05 mg) were placed in the middle of a quartz tube (2 mm diameter and 20 mm long) with a quartz wool base and were then introduced into the platinum Pyroprobe autosampler. Pyrolysis took place at 500 ºC at a heating rate of 20 ºC/ms for 15 s, which were the operational conditions previously optimised elsewhere (Dorado et al., 2020). The experiments were carried out in triplicate for each sample to ensure reproducibility of the obtained chromatograph. The peak area based on the Py-GC/MS analysis could not reveal the real content of the target compounds. If the mass of the sample remained constant during each pyrolysis experiment, the corresponding chromatographs could be compared to reveal any change in its content.

2.5.Data analysis

Statistical analysis was performed through a one-way analysis of variance (ANOVA). A Tukey post hoc test was used to assess statistical differences between the different treated samples, at a significance level of $\alpha = 0.05$, using STATGRAPHICS Centurion (Statgraphics Technologies, Inc.). Different letters represent statistically significant differences for the post hoc Tukey tests performed after each pretreatment, where "a" represents the lowest value and "c" the highest.

3. Results and discussion

3.1.Sample characteristics

The main objective of this paper was to valorise the potential olive pomace (obtained from olive oil in large amounts) had as a subproduct. Thermochemical performance with the fast pyrolysis of any lignocellulosic biomass is closely dependent on its macromolecular composition and mineral content. Thus, its composition could strongly effect the performance of the olive pomace feedstock under fast pyrolysis conditions

(Hernando et al., 2017). Demineralisation techniques could change the lignocellulosic structure of OP, decrease thermal stability and alter the components of the biomass. Therefore, the characterisation study presented herein was applied to the raw OP and to a second batch of de-ashed biomass (obtained with the demineralisation pretreatments dealt with following the procedure described in the experimental section).

Table 1 summarises the main characteristics of OP, before and after pretreatment, including the proximate and ultimate analysis as well as the chemical composition of the raw feedstock, the atomic ratios (H/C and O/C) which resulted, and the high heating value (HHV).

Table 1. Proximate analysis, ultimate analysis, chemical composition and HHV of raw and pretreated OP using demineralisation techniques.

Sample	Proximate analysis (wt.%)*daf				Ultimate analysis (wt.%)*daf				Atomic ratios		HHV (MJ/kg)
	Moisture	Ash	Volatile matter	Fixed carbon*diff	C	H	N	O*diff	H/C	O/C	
OP	2.75±0.05[a]	8.63±0.05[a]	67.05±0.05[a]	24.32	49.06±0.012[a]	8.76±0.012[a]	1.93±0.012[a]	40.25	2.14	0.62	23.07
OP-H_2OT25	4.35±0.05[a]	4.38±0.05[a]	91.32±0.05[a]	4.33	51.12±0.011[a]	6.52±0.011[a]	2.14±0.011[a]	40.14	1.53	0.59	21.25
OP-H_2OT90	4.15±0.05[a]	4.56±0.05[a]	91.32±0.05[a]	4.12	51.20±0.002[a]	6.48±0.002[a]	2.07±0.002[a]	40.15	1.52	0.59	21.23
OP-2.5HCl	3±0.05[a]	2.86±0.05[a]	94.18±0.05[a]	2.96	54.42±0.017[b]	6.86±0.017[b]	2.15±0.017[b]	36.33	1.51	0.50	23.23
OP-5HCl	3.17±0.05[a]	2.75±0.05[a]	94.12±0.05[a]	3.13	53.07±0.045[ab]	6.75±0.045[ab]	2.16±0.045[ab]	37.89	1.53	0.54	22.47
OP-10HCl	3.16±0.05[a]	2.72±0.05[a]	94.15±0.05[a]	3.13	53.64±0.104[c]	6.82±0.104[c]	2.18±0.104[c]	37.23	1.53	0.52	22.82
OP-HNO_3	3.19±0.05[a]	2.35±0.05[a]	94.49±0.05[a]	3.16	52.51±0.034[a]	6.55±0.034[a]	2.24±0.034[a]	38.57	1.50	0.55	21.98
OP-NaOH	4.78±0.05[a]	13.08±0.05[a]	80.77±0.05[a]	6.15	43.91±0.097[b]	5.72±0.097[b]	2.11±0.097[b]	48.20	1.56	0.82	16.77
P-value	<0.001	<0.001	<0.001	-	<0.001	<0.005	<0.005	-	-	-	-

	Chemical composition (wt.%) (*P*-value)		
	Klason lignin	Hemicellulose	Extractives
OP	24.1 ±0.5[a] (0.016)	27.6 ±0.8[b] (0.037)	28.9 ±0.2[a] (0.001)

*daf: dry and ash free basis; O[diff]: % of oxygen calculated from the difference in C, H and N; Fixed carbon[*diff]: % in fixed carbon calculated from difference in ash and volatile matter; *db: dry basis. Data were average of different samples ± standard deviation. Different letters represent statistically significant differences ($p < 0.05$) for the post hoc Tukey tests performed after each pretreatment, where "a" represents the lowest value and "c" the highest.

As shown in Table 1, after water leaching ash content decreased from 8.63% to 4.38%-4.56 wt.% in OP-H_2OT25 and OP-H_2OT90, respectively. Hence 4 wt.% of the ash lost remained as a water-soluble component. As for acid leaching, the ash content fell to 2.86%, 2.75% and 2.72 wt.% in OP with the 2.5%, 5% and 10 wt.% HCl leaching procedures respectively, and the component lost was both water and acid-soluble. Furthermore, this trend concurred with data from OP-HNO_3. Compared to water, acid leaching is more marked and leads to greater loss of organic matter while removing a higher amount of ash simultaneously (Niu et al., 2022). The demineralisation pre-

treatments induced an increase in volatile matter content from 67.05% to over 90 wt.%, while there was a fall in fixed carbon. This was attributed to the removal of inorganic material (metal content) which can catalyse carbonisation when it is in the biomass feedstock (Hernando et al., 2017). In contrast, sodium hydroxide washing was observed to cause impregnation with Na and resulted in a high Na^+ content in the OP-NaOH sample (Li et al., 2022). Thus, ash content in OP-NaOH increased to 13.08 wt.%. However, in OP-NaOH the volatile matter increased due to demineralisation, albeit not to the same extent as with the other leaching procedures used. Furthermore, it has been demonstrated that alkali treatment reduces the mass yield as well as the energy density of the treated OP shown in HHV values (Table 1) (Kumar et al., 2020). Thus, this was attributed to the ash and carbon content lowering the heating value at 16.77 MJ/kg in comparison to the raw OP (23.07 MJ/kg).

Different metals could inherently exist in biomass in different forms. Some of them might be associated with biomass polymers by binding with oxygen-containing functional groups in polymers such as carboxyl groups in cellulose or phenolic groups in lignin (Mayer et al., 2012). The change in metal content in biomass could have influenced catalytic cracking during fast pyrolysis, thus affecting the final bio-oil product distribution. Concentrations of AAEMs in the raw and pretreated olive pomace were measured and compared, as presented in Table 2.

Table 2. AAEM content in raw and pretreated OP using demineralisation techniques, presented with standard deviations

Sample	Mineral content (wt.%)			
	K	Ca	Na	Mg
OP	3.9 ± 0.02^{c}	0.6 ± 0.002^{b}	2.3 ± 0.02^{c}	0.4 ± 0.001^{b}

OP-H_2OT25	0.5 ± 0.001^{b}	0.6 ± 0.002^{c}	1.6 ± 0.02^{c}	0.3 ± 0.001^{c}
OP-H_2OT90	0.3 ± 0.001^{b}	0.5 ± 0.002^{c}	0.04 ± 0.0001^{a}	0.02 ± 0.0001^{a}
OP-2.5HCl	0.01 ± 0.0001^{a}	0.02 ± 0.0001^{a}	0.02 ± 0.0001^{a}	0.1 ± 0.001^{c}
OP-5HCl	0.01 ± 0.0001^{a}	0.01 ± 0.0001^{a}	0.01 ± 0.0001^{a}	0.1 ± 0.001^{c}
OP-10HCl	0.006 ± 0.0001^{a}	0.02 ± 0.0001^{a}	0.005 ± 0.0001^{a}	0.1 ± 0.001^{b}
OP-HNO_3	0.01 ± 0.0001^{a}	0.008 ± 0.0001^{a}	0.05 ± 0.0001^{a}	0.1 ± 0.001^{b}
OP-NaOH	0.6 ± 0.001^{b}	0.6 ± 0.002^{b}	4.2 ± 0.02^{c}	0.4 ± 0.001^{b}

Data were average of different samples ± standard deviation. Different letters represent statistically significant differences ($p < 0.05$) for the post hoc Tukey tests performed after each pretreatment, where "a" represents the lowest value and "c" the highest.

The ICP-OES technique revealed that the most abundant metals in OP were K (3.9 wt.%) and Na (2.3 wt.%). Alkali metals, such as potassium, are known to be important catalysts in biomass pyrolysis. K could have acted as a catalyst during decarbonylation and decarboxylation of the pyrolysis vapors (Wang et al., 2017). After water leaching, most potassium and sodium were removed. This suggests that K and Na in OP are largely water-soluble. Conversely, Ca and Mg are mainly contained in water-insoluble but acid-soluble salts. Alternatively, they could have been associated with organic macromolecules released after acid leaching by means of the io-exchange of the AAEMs with H^{+} (Niu et al., 2022). One striking observation was this solved the natural problem of corrosion caused by the alkali metals (K and Na in this case) in the ash in the bio-oils obtained from the biomass (Kumar et al., 2020). Demineralisation by water leaching was greatly enhanced as treatment temperature rose. Thus, in OP-H_2OT90 the Na and Mg demineralization effect was observed to rise to 98 and 50%, respectively. Ca largely remained in the biomass, showing that water leaching removed hardly any of it unless other leaching solutions were used. The remaining AAEMs in OP were in the form of carboxylate and inorganic minerals which required an acidic medium to remove them (D. Chen et al., 2020). Regarding the HCl treatment, this showed a high removal rate for all

AAEMs even at low concentrations. This was indicative of how effective acid leaching was, albeit slightly lower removal rates were found for HNO_3. Nevertheless, they were still quite high. As for alkali treatment, 86% of K was removed in OP-NaOH. Ca was found to be resistant to alkali washing. Indeed, di-valent species such as Ca are known to be removed more effectively through acid washing pretreatment (Chen et al., 2021). Moreover, Ca in biomass exists not only in the form of calcium carbonate, but also as calcium silicate and other substances which are difficult to dissolve in an organic acid solution (D. Chen et al., 2020). Therefore, as shown in Table 2, acid washing (especially, hydrochloric acid) was essential for removing Ca. Finally, as commented above, sodium hydroxide washing led to an impregnation of Na resulting in a higher Na^+ content in OP-NaOH than in the raw material (an increase of up to 83%).

The elemental composition from the ultimate analysis (Table 1) in terms of C, H, N and O remained fundamentally constant after all pretreatment studies. Fig. 1 shows the Van Krevelen diagram of raw and pretreated OP with the different demineralisation techniques. OP samples with lower O/C and higher H/C ratios were the preferable feedstocks in pyrolysis as they have a higher energy content. From the atomic ratios (Table 1) calculated, it might be concluded that all demineralisation methods decreased O/C and H/C values. This implies oxygenated compounds were removed to a certain extent. This trend varied with the demineralisation techniques used. However, the O/C ratio was lowered to a much larger extent than observed with the H/C ratio in acid leaching OP compared to the raw biomass. This could indicate that carbonates (for which C is also measured in the elemental analysis) in OP react with the acids to form CO_2 in pretreatment, and therefore only lowered the C and O content in the feedstock. In fact, dehydration appears to be one of the most dominant reactions in the water and acid leaching OP samples. This can be seen in the Van Krevelen diagram presented in Fig 1.

The OP-NaOH sample follows a different trend: there is a rise in O/C while the H/C ratio falls in comparison with the raw OP, indicating that oxygenated compounds were enhanced due to the greater amount of metal content (Table 2).

Therefore, pretreatment with different demineralisation techniques may have different effects on fast pyrolysis performance and the product composition of the OP bio-oil in relation to the final composition of AAEMs. As will be discussed below, this will be consistent with variations in compositions of the product.

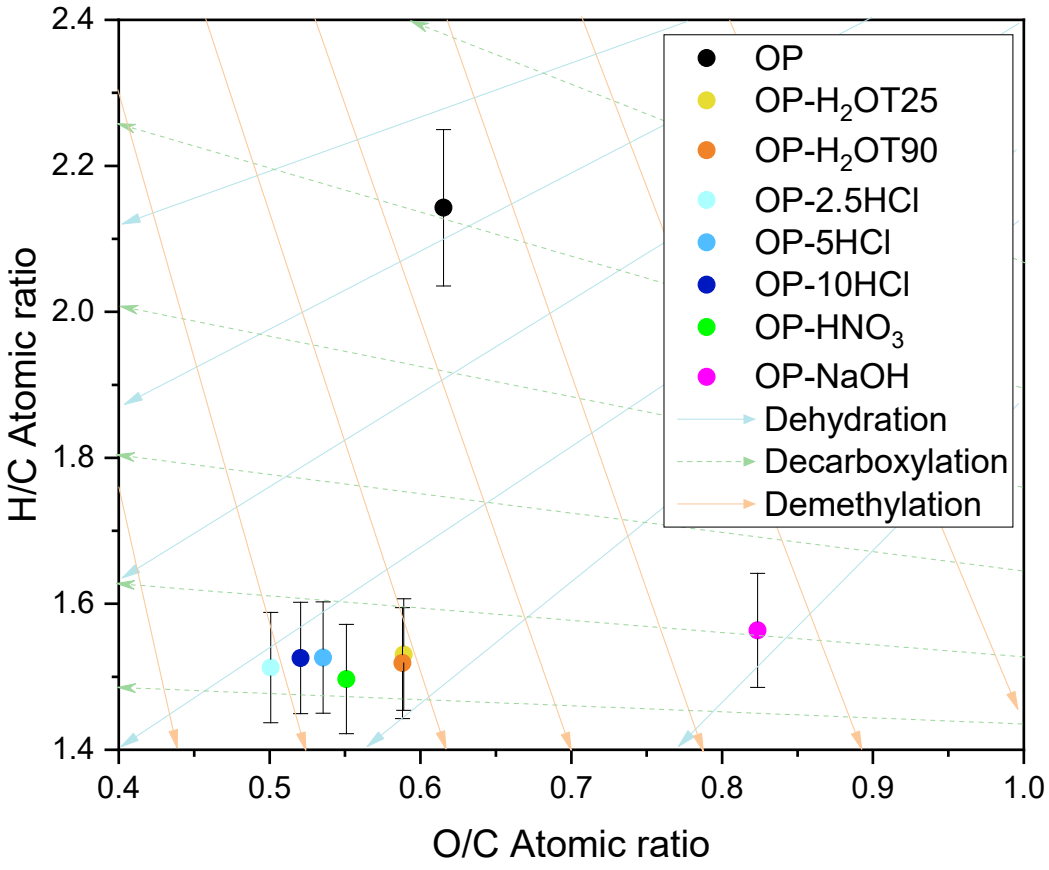

Fig 1. Van Krevelen diagram of raw and pretreated OP using demineralisation techniques.

3.1.1. Thermogravimetric analysis

The thermal performance for raw OP and pretreated samples in an inert atmosphere was determined by thermogravimetric tests whose results and corresponding DTG curves are displayed in Fig. 2.

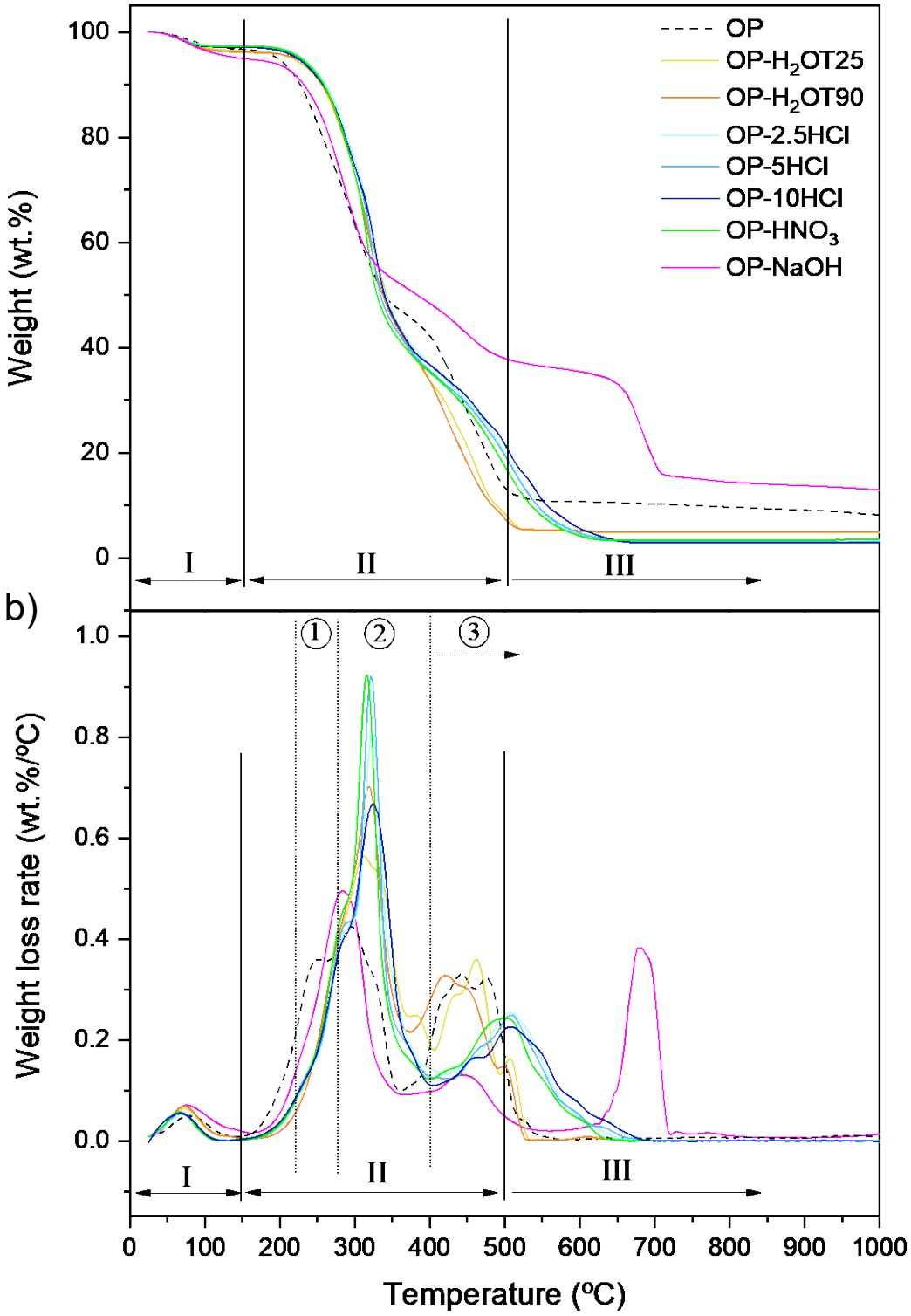

Fig 2. Thermogravimetric analysis, a) TG and b) DTG curves for raw and pretreated OP using demineralisation techniques.

The main pyrolysis step for the biomass samples took place at temperatures between 120 and 450 ºC, as can be seen from their DTG profile. The pyrolysis was divided into three common degradation stages: water drying/evaporation (stage I: 0-150 ºC), devolatilisation (stage II: 150-500 ºC) and char formation (stage III: >500 ºC) (Puig-Gamero et al., 2020). Moreover, a small peak was observed at around 400 ºC for the OP which was linked to lipid decomposition in the olive oil (Puig-Gamero et al., 2020). As for the demineralised samples, significant differences could be observed on the DTG curves from those in the raw OP. These were related to the change in physical structure and chemical composition after the corresponding pretreatments. As shown in Fig. 2 at stage II, the DTG curves for the raw OP and treated samples tended to display a clear shoulder. This indicated that these DTG curves overlapped at two peaks (named 1 and 2): Peak 1 was mainly attributed to the decomposition of the thermally labile hemicellulose, and peak 2 was largely due to the decomposition of cellulose. After water and acid leaching pretreatments, both peak 1 and 2 shifted to higher temperatures. This could be explained by the fact that some AAEMs inherent in the OP that acted as catalysts had been removed (Jiang et al., 2013b). Stage 3 corresponded to lignin decomposition and carbonisation. This indicated that lignin has high thermal stability due to its highly cross-linked structure. The loss in mass observed at temperatures above 600 ºC was ascribed to the decomposition of endogenous inorganic salts (Niu et al., 2022). This loss in mass was significantly observed in the NaOH treated sample, which thermally decomposed at higher temperatures. However, stages 1 and 2 with the OP-NaOH sample were combined into one decomposition stage which could imply significant changes in the lignocellulosic structure of the sample.

According to the TG/DTG results, pretreated samples showed a higher content of higher volatiles than seen in the raw OP. Thus, these materials showed potential for being converted into bio-oil by fast pyrolysis (Braga et al., 2021).

3.1.2. Surface functional groups evolution

To obtain more information on the differences in chemical structure in the raw OP and demineralised samples, FTIR measurements were conducted. The infrared absorption spectra for the OP and pretreated samples were plotted against the wavenumber in Fig. 3. With this technique we obtained a correlation with functional groups such as alkenes, esters, aromatics, ketones and alcohols, among others in the biomass samples. In general, the IR spectra for the samples after undergoing different demineralisation techniques showed similar patterns, but minor changes in surface chemical functional groups were still observed due to hydrolysis that occurred during pretreatment.

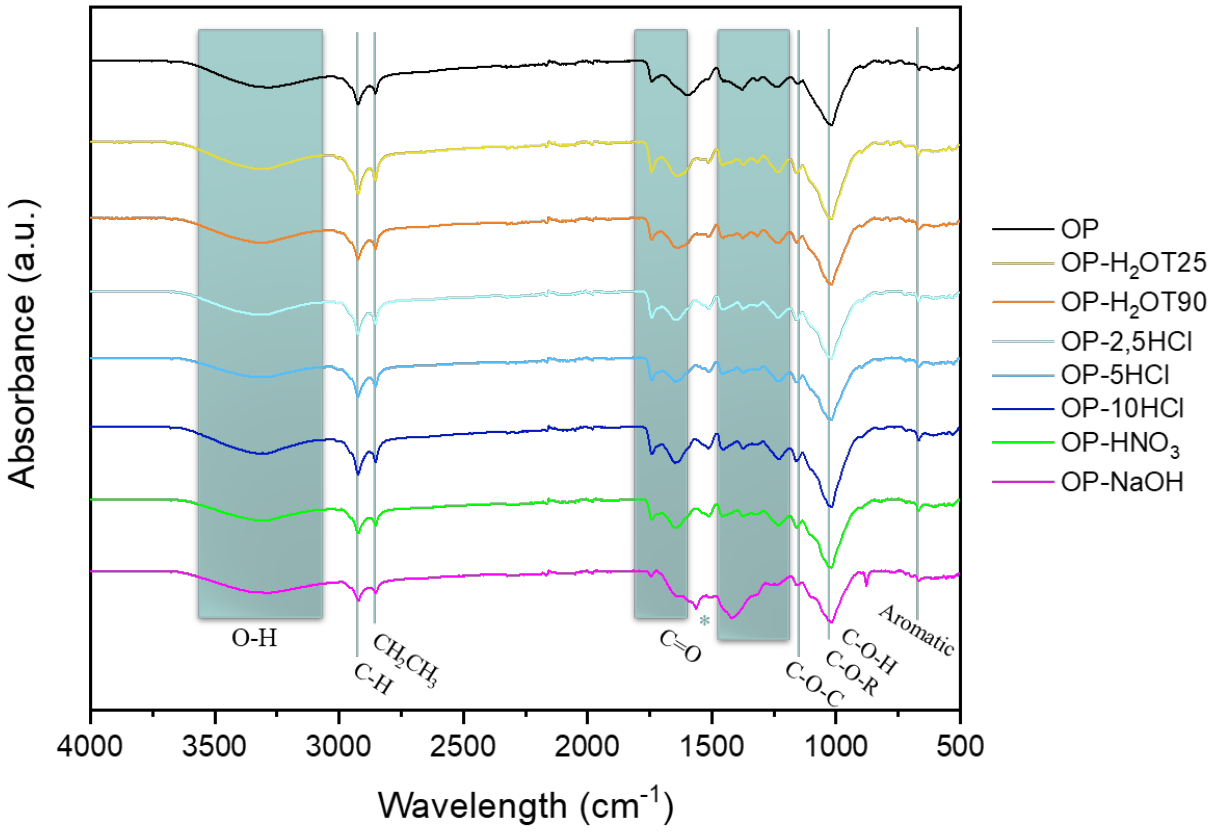

Fig 3. FTIR spectra for raw and pretreated OP using demineralisation techniques.

In the mid-infrared spectra, the first dominant broad band at 3000-3600 cm^{-1} was attributed to an O-H stretching vibration of the hydroxyl functional groups in phenolic and alcoholic compounds. The band at 2800-3000 cm^{-1} was associated with C-H stretching vibrations of the CH_2 and CH_3 groups in the lignin structure (Fan et al., 2017). The adsorption intensities of bands near 1730 cm^{-1} (which are assigned to C=O stretching of esters and fatty acids) slightly increased after demineralisation. This concurs with Liu et al. (2019) and Niu et al. (2022) who suggested that the fatty acid methyl esters content could increase under acidic conditions. Therefore, it is typically a hemicellulose marker. The opposite is true with the sodium hydroxide leach sample in which the slightly narrower band suggest acid production had reduced. The band at around 1650 cm^{-1} only appeared in OP-NaOH. In the literature, this is the result of the joint stretching vibration of the aromatic ring associated with lignin and carbonate impurities (Jiang et al., 2013b; M.R., 1981). The peaks in the 1440-1380 cm^{-1} region corresponded to asymmetric bending of the lignin structure linked to the aromatic groups stretching and breathing vibrations from syringyl units in the lignocellulosic biomass (Dorado et al., 2020; Li et al., 2022). The -OH links in the aromatic nucleus are located at 1377 cm^{-1}, and the C-O and -OCH_3 in the guaiacyl nucleus at 1268 cm^{-1} (Huang et al., 2020a). These gradually became more intense in the demineralised sample, especially in OP-NaOH. Moreover, the stretching band at 1250 cm^{-1} could have been related to the presence of C-O-C in the cellulose biopolymer chain. The spectra between 1100 and 900 cm^{-1} showed a high intensity peak which was related to C-O-H stretching vibration links. These were probably cellulose and hemicellulose-related absorptions or due to the presence of C-O-R alcohols or esters (Fan et al., 2017). These bands tapered as a great deal of acid leaching

was concentrated in OP. Finally, the peak at around 600 cm^{-1} was associated with bending modes of aromatic compounds (X. Chen et al., 2019b).

According to the results, it is remarkable that alkali treatment with NaOH could enhance -OH links in the aromatic substances and C-O and -OCH_3 in the guaiacyl compounds in the lignin structure.

3.2. Effects of demineralisation techniques on fast pyrolysis bio-oil composition

The presence of AAEMs inherent in the biomass organic matrix is known to promote dehydration of the holocellulose matrix, favouring ring opening reactions from the carbohydrate oligomers. These could also catalyse rupture of ether bonds and side-chains units inside the lignin matrix, and promote deoxygenation of biomass structures through decarboxylation, decarbonylation, dihydroxylation and demethylation (Giudicianni et al., 2021). In this section, there is an analysis of how the AAEMs removed after demineralisation affected the bio-oil composition in the raw OP and pretreated samples through fast pyrolysis. To better understand the results, we should stress that the OP sample was oily and contained high amounts of water-soluble fats, carbohydrates and phenolics (Dorado et al., 2020; Volpe et al., 2014) and this greasy character could have strongly determined the bio-oil composition obtained with fast pyrolysis.

3.2.1. Effect of water leaching on olive pomace with fast pyrolysis

Olive pomace was pretreated with water leaching at two different temperatures, room (25 ± 3 ºC) and 90 ºC, to show the effect of removing AAEMs on final product distribution after fast pyrolysis. Fig 4. shows the bio-oil product distribution with fast pyrolysis of raw and water leached OP samples. The products detected were separated as the functional groups of alcohols, cyclic hydrocarbons, aldehydes, alkanes, carboxylic acids, ketones, esters, nitrogenates and phenolic compounds.

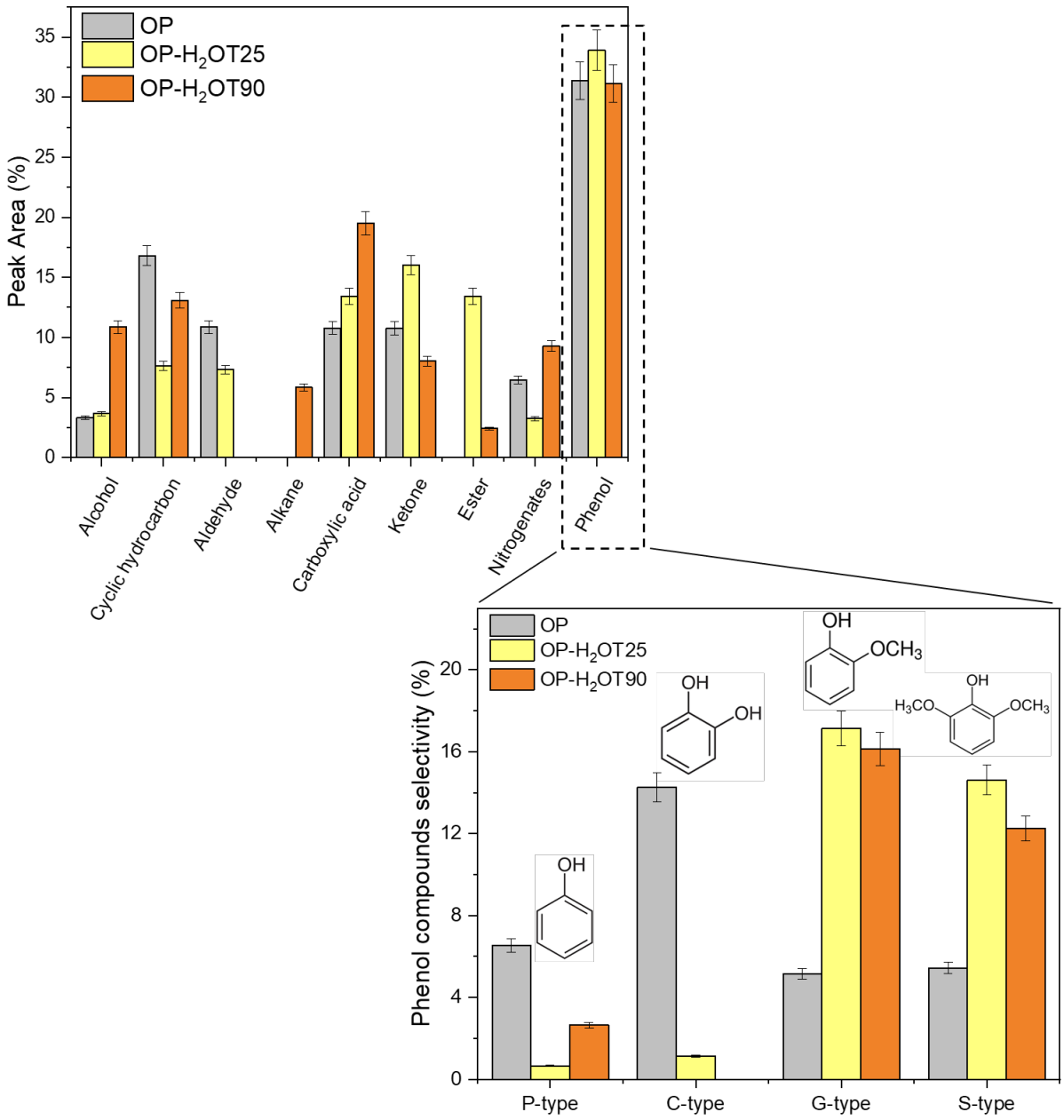

Fig 4. Bio-oil products and phenolic compounds distribution for OP with fast pyrolysis water leaching pretreated at room temperature (OP-H_2OT25) and 90ºC (OP-H_2OT90).

Through water leaching, the bio-oil obtained in OP-H_2OT25 showed an increase in the proportion of oxygenates, accompanied by a reduction in hydrocarbons and nitrogenous compounds. Nonetheless, the proportion of oxygenates obtained in OP-H_2OT90 decreased to yields representing 71.8% of the composition, and hydrocarbon compounds increased slightly to yields representing 18.9 %, all of which were in comparison to the

raw OP. As seen in Fig. 4, the composition of the bio-oil obtained during fast pyrolysis was influenced by the demineralisation pretreatment temperature. This trend was closely related to rates of demineralisation (Table 2). The higher the temperature in pretreatment, the more efficient demineralisation became. As for the efficiency of removing K, this was similar in both pretreatments, but different yields were obtained for Na which were 30% and 98% in OP-H_2OT25 and OP-H_2OT90, respectively. As the pretreatment temperature rises, hemicellulose is known to be largely removed and lignin slightly removed (Kumar et al., 2020). Thus, the most representative functional group obtained was phenols and their derivatives which reached maximum yields of 30% from the decomposition of chemical bonds in the lignin (Kumar et al., 2021). These compounds were obtained in the same range in both water leaching samples. Hence, this confirms that the catalytic effect of removing metal had no influence on the formation of oxygenated compounds from lignin cracking and ring opening in hemicellulose structures (Alcazar-Ruiz et al., 2021). However, the OP sample contained a relatively high proportion of olive oil, which decomposed to form light carboxylic acids, alcohols, and olefins after fast pyrolysis. Carboxylic acids (mainly acetic acid), and alcohol compounds were enhanced with the water leached samples and the highest yields were obtained in OP-H_2OT90. Moreover, removing potassium could have prevented long-chain fatty acids from decomposing (Hu et al., 2021). In addition, these trends were related to the high amount of alkali metals removed in comparison with OP-H_2OT25, and the presence of alkaline earth metals (like Ca^{2+}). The latter promoted ring scission, isomerisation, and dehydration with the cellulose (Alcazar-Ruiz et al., 2021; Giudicianni et al., 2021). Few hydrocarbon compounds were obtained due to the limited amount of inorganic compounds left after water leaching promoted cracking and deoxygenation (D. Chen et al., 2019).

A more detailed study was carried out on the phenolic compounds detected, as they were the main functional group obtained. According to the different oxygen-containing substituted groups (hydroxyl (-OH) and methoxyl (-OCH_3)) linked to the benzene ring, the phenolics obtained were distributed into four types of components: i) phenol type (P-type) which contained only one hydroxyl, ii catechol type (C-type) which contained two hydroxyls, iii) guaiacol type (G-type) which contained one methoxyl and one hydroxyl, and iv) syringol type (S-type) which contained two methoxyl and one hydroxyl substituted groups. This concurred with other research (Huang et al., 2020b; M. Huang et al., 2021). The phenolic yields detected from OP bio-oil with fast pyrolysis were: 6.54% P-type, 14.25% C-type, 5.14% G-type and 5.43% S-type. Among all the phenolics, phenol (4% P-type), Benzeneethanol, 4-hydroxy (8.86% C-type), 3-tert-Butyl-4-hydroxyanisole (3.84% G-type) and Phenol, 2,6-dimethoxy (4.71% S-type) were found to be the main phenolics obtained from the raw OP with fast pyrolysis. Table S1 gives a detailed breakdown of phenolics distribution from the bio-oils produced by the raw OP and pretreated fast pyrolysis samples. As seen in Fig. 4, the G-type and S-type after fast pyrolysis of the water leached sample were promoted more in comparison with the raw OP. With the S-type, the maximum was reached with OP-H_2OT25 in which syringol (Phenol, 2,6-dimethoxy) and 4-(prop-1-en-1-yl) syringol ((E)-2,6-Dimethoxy-4-(prop-1-en-1-yl) phenol) represented 5.36% and 5.1% yields, respectively. However, G-type yields were in the same range in the water leached samples in which the most representative compound was (E)-4-(3-Hydroxyprop-1-en-1-yl)-2-methoxyphenol. Guaiacol (Phenol, 2-methoxy) was produced in OP-H_2OT25 with a yield of 3.4%, and 4-vinyl-guaicol (2-Methoxy-4-vinylphenol) was largely produced in both water leaching samples which reached yields of 2.8% and 4.5 % in OP-H_2OT25 and OP-H_2OT90 respectively. This demineralisation technique revealed how important K was as a catalyst

(a large amount was removed through both water leaching processes) which induced hydrolysis of -OCH_3 and promoted demethoxylation, enhancing C-type formation (M. Huang et al., 2021; Kumar et al., 2021). Leaching OP with deionised water is an easy, efficient and cost-effective technique which enhances selective production of guaiacol (Phenol, 2-methoxy) in OP-H_2OT25 and syringol (Phenol, 2,6-dimethoxy) in OP-H_2OT90.

3.2.2. Acid leaching effect on olive pomace with fast pyrolysis

Biomass pretreatment with diluted acidic chemicals have been considered as a beneficial technique for removing inorganic species which could initiate polymerisation or condensation that is highly detrimental to bio-oil stability (Kumar et al., 2020). Raw olive pomace was pretreated with two different acidic solutions, HCl and HNO_3. With the former, three different concentrations (2.5%, 5% and 10 wt.%) were used to study its effect on the final bio-oil composition. Another acidic agent (HNO_3 leaching) was used to reveal differences in bio-oil composition depending on the acid solution used. The main chemical species in the bio-oil obtained from fast pyrolysis of OP-HCl and OP-HNO_3 are shown in Fig. 5.

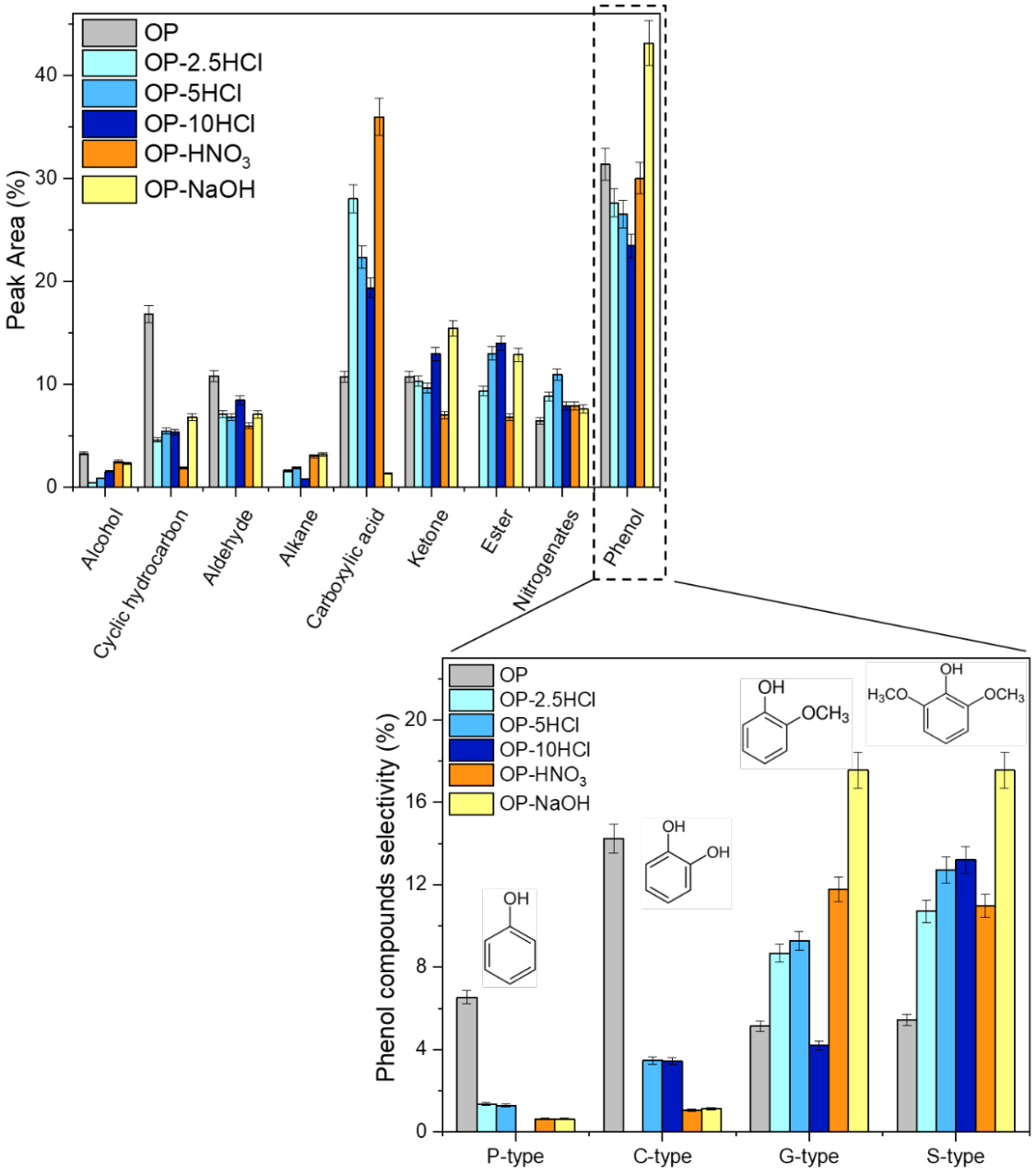

Fig 5. Bio-oil products and phenolic compounds distribution of fast pyrolysis OP acid (OP-2.5HCl, OP-5HCl, OP-10HCl and OP-HNO_3) and pretreated alkali leaching (OP-NaOH).

Oxygenates were dominant in the bio-oil derived from the acid leached OP samples and there was an insignificant fraction of hydrocarbons in comparison to those found in the raw OP. The acid leached samples produced an increase in oxygenate compounds from yields of 76.3% to 85.5% in OP and 88.4% in OP-10HCl and OP-HNO_3, respectively.

However, acid leaching resulted in an increase in the yield of nitrogenated compounds. They showed slight increases after acidic pretreatments, especially with HNO_3 leaching, which displayed yields of 8%. The trends observed were related to highly efficient demineralisation. With acid leaching, nearly 100% of the metals were removed and only Mg had a slight resistance to the leaching. Again, phenolic compounds, followed by carboxylic acids (both typically obtained through fast pyrolysis of olive pomace) were the main functional groups obtained. However, in terms of phenolics, yields fell as the concentration of HCl solution rose. This was associated with the strong demethoxylation in acid leaching, which caused the $-OCH_3$ bond in the lignin structure to be removed by cleavage (Duan et al., 2019). Specifically, the relative proportion of phenolics decreased from 31.4% to 23.5% in the raw OP and OP-10HCl, respectively. Acid leaching also promoted the devolatilisation of the lignin in OP by suppressing carbonisation during pyrolysis (Khan et al., 2021). Moreover, carboxylic acids production was promoted, especially in OP-HNO_3. Results revealed that with acetic acid, yields of 15% were obtained in sample OP-2.5HCl. The hemicellulose was partially hydrolysed during acid washing and interactions with holocellulose content fell whilst those with lignocellulosic content rose. This led to a rise in levoglucosan and carboxylic production as the samples underwent pyrolysis (Khan et al., 2021). Thus, yields of carboxylic acid came to 32% in OP-HNO_3. With the different HCl leachings, acid yields at first rose to 28% in OP-2.5HCl before falling steadily to reach a yield of 19.4% as the concentration of the HCl solution rose. This trend was associated with carboxylic acids production that had been seen previously in the FTIR analysis (Fig. 3). As mentioned above, there was a decline in hydrocarbon compounds with acid leaching. However, production of aromatic hydrocarbons, mainly toluene, increased (1% and 2.5% in OP-5HCl and OP-10HCl, respectively).

A detailed comparison was made for the different types of phenols detected. In general, production of lighter phenols such as the P-type and C-type were limited whereas yields of the G-type and S-type increased. It has also been proven that acid treatment of lignocellulose biomass promotes formation of certain organic compounds such as vinyl-guaiacol and syringol which are mainly derived from thermal degradation of lignin. This indicated *αC-βC* bonds and *β-5* bonds in the lignin structure were broken after acidic treatment (Kumar et al., 2020). In the G-type, (E)-4-(3-Hydroxyprop-1-en-1-yl)-2-methoxyphenol was obtained in large amounts with yields rising in tandem with increases in acidic leaching, showing a 4.2% yield in OP-10HCl. A yield of 2.9% for 4-yinyl-guaiacol (2-Methoxy-4-vinylphenol) was obtained in OP-HNO_3. With the S-type, yields increased from 10.7%, 12.7%, and 13.2% in OP-2.5HCl, OP-5HCl and OP-10HCl, respectively. In OP-HNO3, the S-type had a yield of 11%. The most important compound detected was syringol which peaked at 3.4%, 3.3%, 2.9%, and 3.3 % in OP-2.5HCl, OP-5HCl, OP-10HCl and OP-HNO_3 respectively.

The greatest differences were observed with HCl and HNO_3 pretreatments in the distribution of carboxylic acid as well as phenolic compounds. Consequently, it should be noted that yields of organic compounds in the pyrolytic bio-oil was greatly influenced by the type and concentration of acidic solvent used in demineralisation.

3.2.3. Alkali pretreatment with fast pyrolysis of olive pomace

Alkaline pretreatment of biomass enables the lignin to be removed and cellulose digestibility is enhanced (Kumar et al., 2020). Moreover, this could cause the ester and glycosidic links in the lignin structure to break. The results obtained in OP-NaOH also revealed that NaOH treatment increased the amount of hemicellulose and lignin (Fig. 2). Thus, this implies an increase in lignin-pyrolysed compounds, such as phenolic compounds, in the bio-oil. As shown in Table 2, during alkali pretreatment, the hydroxide

anion and the sodium cation dissociate and the increased concentration of hydroxide ions is directly proportional to the rate of hydrolysis (Kim et al., 2016). This could explain how the proportion of oxygenate compounds detected in the fast pyrolysis of OP-NaOH bio-oil increased from a yield of 76.3% in the raw OP to 82.3% (see Fig. 5). Consequently, the proportion of hydrocarbon compounds (most of which were cyclic hydrocarbons) decreased. As shown in Fig. 5, the product distribution of the bio-oil obtained enhanced production of phenolic compounds to a yield of 43.2% while carboxylic acid (largely obtained in OP due to its greasy nature) dropped to a yield of 1.3%. From the FTIR results (Fig. 3), carboxylic acids production was estimated to fall after alkali pretreatment. Treatment with NaOH was found to depolymerise the lignin into phenolic monomers and dimers and prevented it agglomerating during pyrolysis (Giudicianni et al., 2021). Noticeably, P-type and C-type phenols fell in comparison with the raw OP, enhancing production of the G-type and S-type to yields of 17.6% and 17.7%, respectively. However, with the G-type, promotion of guaiacol (Phenol, 2-methoxy) and 4-vinyl-guaicaol (2-Methoxy-4-vinylphenol) was observed with yields of 6% and 6.3%, respectively. Na^+ enhanced removal of methoxy and hydroxyl groups from different types of pulp lignin, determining an increase in yields of guaiacol and vinyl guaiacol and a decrease in those of methyl guaiacol (Giudicianni et al., 2021). With the S-type, syringol (Phenol, 2,6-dimethoxy) was enhanced to a yield of 11% in comparison to the raw OP.

Among the demineralisation techniques carried out in this study, alkali leaching using NaOH showed a good rate of K removal and sound performance in terms of phenolic distribution. Therefore, this alkali pretreatment could be used to enhance yields of valuable phenolic compounds such as guaiacol and syringol from the olive pomace. This is of great interest, as they are valuable products. Guaiacol could be used as a model compound, a carbon-based starting material, plant nutrient, functional solvent in

pharmaceuticals, pesticide, fragrance, and in cosmetics and other industries (Chen et al., 2022; Huang et al., 2021; Torres et al., 2021). It has been proved that guaiacol production is not only significance scientifically but also economically too (Feng et al., 2018). Regarding syringol, this could be used in the pharmaceutical sector in platelet aggregation and for anti-dermatophyte activity (Curmi et al., 2022).
In short, it represents an outstanding opportunity to obtain a large amount of renewable phenolic monomers (guaiacols, 4-ethylguaiacol and syringol) from a waste biomass such as olive pomace (Campos-Franzani et al., 2020).

Finally, Table 3 summarises the results from different research on the effects of similar demineralisation pretreatments as those used in this work, for different types of lignocellulosic biomass and on phenolic yields obtained from pyrolytic bio-oils. It has also been observed that these yields tended to decrease after demineralisation, especially from acid leaching. However, for alkali pretreatments with NaOH, increasing yields of phenolics were observed depending on the biomass feed. Nevertheless, there must be an in-depth characteristic analysis of the biomass feed to be treated. Depending on its chemical composition, the degree of demineralisation from each pretreatment used and the predominance of the deoxygenation route taken by fast pyrolysis, the quality and distribution of phenolic compounds in the bio-oil obtained will change. However, the results reported confirm the trends obtained with the demineralisation techniques used in our study.

3.3. Demineralisation effect on deoxygenation selectivity

The major reaction pathways during fast pyrolysis of biomass are ketonisation, catalytic cracking, aldol condensation, aromatisation and deoxygenation (Kabir and Hameed, 2017). Deoxygenation is a promising route for enhancing bio-oil quality by removing oxygenated compounds in the form of CO, CO_2 and H_2O by decarbonylation,

decarboxylation and dehydration respectively (Dada et al., 2021). Selectivity for these three deoxygenation pathways with the demineralised olive pomace samples is shown in Fig. 6. The compounds formed related to water formation during the reaction are grouped as dehydration pathways. For decarboxylation and decarbonylation, they are calculated as the sum of the functional groups that contributed to CO and CO_2 formation respectively (Alcazar-Ruiz et al., 2021; Fermoso et al., 2017).

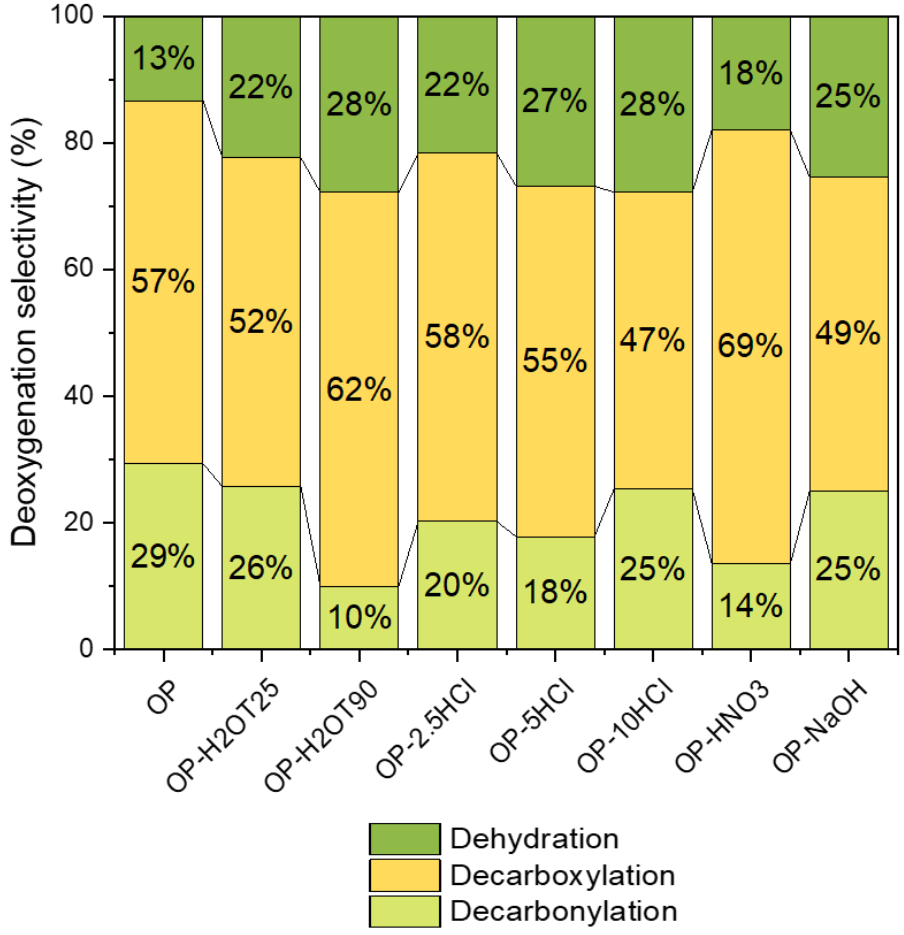

Fig 6. Deoxygenation selectivity obtained from the bio-oil fast pyrolysis of raw and pretreated OP samples.

Mineral content plays a key role in deoxygenation and production of selective bio-oil compounds (Dada et al., 2021). Fig. 6 exhibits deoxygenation selectivity for the oxygen-containing compounds obtained through fast pyrolysis with the demineralised techniques.

In general, demineralised samples with a smaller number of inorganic species while decarbonylation pathways fall, hence decreasing emissions in the form of CO_2 from oxygen-containing gaseous components. CO_2 was mainly produced from decarbonylation at the end group of the side-chain in phenylpropyl structural units (Xu et al., 2019). However, decarbonylation and decarboxylation were promoted by the catalytic action of AAEMs, mainly K, thereby increasing the proportion of light oxygenated compounds from hemicellulose and cellulose (Leng et al., 2017). This was observed in OP-H_2OT90, in which a large amount of K was removed. As previously mentioned, in the Van Krevelen diagram (Fig. 1), water and acid pretreatments promoted dehydration to form H_2O. However, acid leaching indicated that the carbonated fraction of OP reacted with acid solvents to form CO_2. This trend was observed in Fig. 6, with enhanced decarbonylation with the acid concentration. In contrast, HNO_3 pretreatment led to a fall in decarbonylation, as the drop in oxygen (given by the elemental analysis, Table 1) was not as acute as with HCl. The CO produced from the decarboxylation of oxygenated compounds mainly came from the breakage of the aryl ether bond (β-O-4 and α-O-4) (Huang et al., 2020a). With OP-NaOH, sodium content increased to 83% (see Table 2), thus exciting hydrogen bonds in hydroxyl groups and promoting dehydration.

Table 3. Effect of water, acid and alkali pretreatment on phenolic yields of the pyrolytic bio-oil.

Type of lignocellulosic biomass	Demineralisation solution	Pyrolysis temperature (ºC)	Phenolic yields (%)		Key findings	Ref.
			Raw	Pretreated		
Corn straw	0.1 mol/l HCl	500	24	19	During the pyrolysis of lignin, the fracture of carbon-carbon and ether bonds will produce phenol compounds. A slight reduction in the *2-methoxy-4-vinylphenol* absolute peak area appeared after HCl washing.	(Chen et al., 2021)
Rice straw	Deionised water	400-750	35	28	Water-soluble alkali metals had a positive effect on the formation of phenols, while ion-exchanged alkali and acid- soluble alkali metals showed a negative influence on phenol production at 750 ◦C.	(Zhang et al., 2022)
	HCl			22		
Elephant grass	Hot water, 60ºC	600	30	23	The rise in phenols could have been due to the protons K^+ and H^+ from the water treated sample inducing hemolytic	(Braga et al., 2021)

					scissions of cellulose and consequently formations of non-methoxylated phenols and C_1–C_3 compounds.	
	HCl			27	-	
Nannochloopsis gaditana (marine microalgae)	Water at 25ºC	500	2.4	3.6	Since there is no lignin in microalgae, the phenols and aromatic hydrocarbons are formed from proteins and lipids.	(Niu et al., 2022)
	HCl			4.2		
Loblolly Pine	NaOH (0.5 wt.%)	450	4.4	3.2	The quality of bio-oil obtained was determined based on HHV, water content, pH, and viscosity	(Wang et al., 2011)
Napier Grass	Ultrapure water, 25ºC	600	30.6	37.4	-	(Mohammed et al., 2017)
	NaOH			39.5		
Tobacco stem	HCl (3 wt.%)	450	Lower yields than those in raw sample			(Li et al., 2022)

NaOH (3 wt.%)	Enhanced formation accompanied by aldehydes and ketones components	Polyphenols comes from low boiling point no-polymeric components from tobacco

4. Conclusion

This research has shown that the demineralisation pretreatment for olive pomace could be a promising approach for obtaining an enriched phenolic bio-oil through fast pyrolysis. Results indicated that changes in metal content due to pretreatment techniques could influence catalytic cracking during fast pyrolysis. This affected the final bio-oil product distribution.

Pretreated samples displayed a higher volatile content than the raw feed. This indicated they had potential to be converted into bio-oil by fast pyrolysis. Dehydration was identified as the main reaction pathway for water and acid leaching, while alkali pretreatment enhanced oxygenated production due to the rise in of Na^+ content.

The higher the temperature in water leaching pretreatment, the more efficient demineralisation becomes. C-type and S-type phenolic compounds were promoted after fast pyrolysis of water leached samples due to the reduction in K content. Thus, guaiacol in OP-H_2OT25 and syringol in OP-H_2OT90 had yields of 3.4% and 4.4%, respectively.

Acid leaching removed nearly 100% of metal content. Yields of phenolics decreased as the concentration of HCl in the solution rose. Significant differences were observed in carboxylic acid distribution and, also, in phenolic compounds with HCl and HNO_3 pretreatments. Production of lighter phenols such as the P-type and C-type were limited whereas yields of the G-type and S-type rose. Syringol was the main phenolic compound detected.

As for alkali pretreatment with NaOH, sodium content in the sample increased by 83%, which enhanced removal of methoxy and hydroxyl groups from different types of pulp lignin. Therefore, owing to the Na content in the sample guaiacol and vinyl guaiacol

selectivity was enhanced and there was a fall in yields of methyl guaiacol. Remarkably, syringol (S-type) was obtained with a yield of 11%.

CRediT authorship contribution statement

A. Alcazar-Ruiz: Conceptualization, Investigation, Writing - original draft, Data curation, Supervision. **F. Dorado**: Format analysis, Methodology, Funding acquisition, Writing - review & editing. **L. Sanchez- Silva**: Validation, Resources, Writing - review & editing.

Acknowledgements

The authors wish to thank the regional government of Castilla -La Mancha for their financial support (Project SBPLY/17/180501/000238).

List of References

Alcazar-Ruiz, A., Dorado, F., Sanchez-Silva, L., 2021. Fast pyrolysis of agroindustrial wastes blends: Hydrocarbon production enhancement. J. Anal. Appl. Pyrolysis 157, 105242. https://doi.org/10.1016/j.jaap.2021.105242

Alcazar-Ruiz, A., Garcia-Carpintero, R., Dorado, F., Sanchez- Silva, L., 2021. Valorization of olive oil industry subproducts: ash and olive pomace fast pyrolysis. Food Bioprod. Process. 125, 37–45. https://doi.org/https://doi.org/10.1016/j.fbp.2020.10.011

Alcazar-Ruiz, A., Ortiz, M.L., Sanchez-Silva, L., Dorado, F., 2021. Catalytic effect of alkali and alkaline earth metals on fast pyrolysis pre-treatment of agricultural waste. Biofuels, Bioprod. Biorefining 1–12. https://doi.org/10.1002/bbb.2253

Braga, R.M., Melo, D.M.A., Melo, M.A.F., Freitas, J.C.O., Boateng, A.A., 2021. Effect of pretreatment on pyrolysis products of Pennisetum purpureum Schum. by Py-

GC/MS. J. Therm. Anal. Calorim. https://doi.org/10.1007/s10973-021-11025-5

Campos-Franzani, M.I., Gajardo-Parra, N.F., Pazo-Carballo, C., Aravena, P., Santiago, R., Palomar, J., Escalona, N., Canales, R.I., 2020. Extraction of guaiacol from hydrocarbons as an alternative for the upgraded bio-oil purification: Experimental and computational thermodynamic study. Fuel 280, 118405. https://doi.org/10.1016/J.FUEL.2020.118405

Chen, D., Cen, K., Chen, F., Ma, Z., Zhou, J., Li, M., 2020. Are the typical organic components in biomass pyrolyzed bio-oil available for leaching of alkali and alkaline earth metallic species (AAEMs) from biomass? Fuel 260, 116347. https://doi.org/10.1016/J.FUEL.2019.116347

Chen, D., Gao, D., Huang, S., Capareda, S.C., Liu, X., Wang, Y., Zhang, T., Liu, Y., Niu, W., 2021. Influence of acid-washed pretreatment on the pyrolysis of corn straw: A study on characteristics, kinetics and bio-oil composition. J. Anal. Appl. Pyrolysis 155, 105027. https://doi.org/10.1016/j.jaap.2021.105027

Chen, D., Wang, Y., Liu, Y., Cen, K., Cao, X., Ma, Z., 2019. Comparative study on the pyrolysis behaviors of rice straw under di ff erent washing pretreatments of water , acid solution , and aqueous phase bio-oil by using TG-FTIR and Py-GC / MS. Fuel 252, 1–9. https://doi.org/10.1016/j.fuel.2019.04.086

Chen, M., Tang, Z., Wang, Y., Shi, J., Li, C., Yang, Z., Wang, J., 2022. Catalytic depolymerization of Kraft lignin to liquid fuels and guaiacol over phosphorus modified Mo/Sepiolite catalyst. Chem. Eng. J. 427, 131761. https://doi.org/10.1016/J.CEJ.2021.131761

Chen, X., Che, Q., Li, S., Liu, Z., Yang, H., Chen, Y., Wang, X., Shao, J., Chen, H., 2019a. Recent developments in lignocellulosic biomass catalytic fast pyrolysis :

Strategies for the optimization of bio-oil quality and yield. Fuel Process. Technol. 196, 106180. https://doi.org/10.1016/j.fuproc.2019.106180

Chen, X., Che, Q., Li, S., Liu, Z., Yang, H., Chen, Y., Wang, X., Shao, J., Chen, H., 2019b. Recent developments in lignocellulosic biomass catalytic fast pyrolysis: Strategies for the optimization of bio-oil quality and yield. Fuel Process. Technol. 196, 106180. https://doi.org/10.1016/J.FUPROC.2019.106180

Chen, Y., Luo, Z., Fang, M., Wang, Q., 2020. Migration and transformation of sodium during staged coal combustion of Zhundong coal and influence of carbon coating. Fuel Process. Technol. 203, 106382. https://doi.org/10.1016/j.fuproc.2020.106382

Curmi, H., Chirat, C., Roubaud, A., Peyrot, M., Haarlemmer, G., Lachenal, D., 2022. Extraction of phenolic compounds from sulfur-free black liquor thanks to hydrothermal treatment before the production of syngas for biofuels. J. Supercrit. Fluids 181. https://doi.org/10.1016/j.supflu.2021.105489

Dada, T.K., Sheehan, M., Murugavelh, S., Antunes, E., 2021. A review on catalytic pyrolysis for high-quality bio-oil production from biomass. Biomass Convers. Biorefinery. https://doi.org/10.1007/s13399-021-01391-3

Dorado, F., Sanchez, P., Alcazar-Ruiz, A., Sanchez-Silva, L., 2020. Fast pyrolysis as an alternative to the valorization of olive mill wastes. J. Sci. Food Agric. https://doi.org/10.1002/jsfa.10856

Duan, D., Dong, X., Wang, Q., Zhang, Y., Ruan, R., Wang, Y., Lei, H., 2021. Production of renewable phenols from corn cob using catalytic pyrolysis over self-derived activated carbons prepared with torrefaction pretreatment and chemical activation. Colloids Surfaces A Physicochem. Eng. Asp. 623, 126507. https://doi.org/10.1016/j.colsurfa.2021.126507

Duan, D., Lei, H., Wang, Y., Ruan, R., Liu, Y., Ding, L., Zhang, Y., Liu, L., 2019. Renewable phenol production from lignin with acid pretreatment and ex-situ catalytic pyrolysis. J. Clean. Prod. 231, 331–340. https://doi.org/10.1016/j.jclepro.2019.05.206

Ducom, G., Gautier, M., Pietraccini, M., Tagutchou, J.P., Lebouil, D., Gourdon, R., 2020. Comparative analyses of three olive mill solid residues from different countries and processes for energy recovery by gasification. Renew. Energy 145, 180–189. https://doi.org/10.1016/j.renene.2019.05.116

Fan, L., Zhang, Y., Liu, S., Zhou, N., Chen, P., Cheng, Y., Addy, M., Lu, Q., Omar, M.M., Liu, Y., 2017. Bio-oil from fast pyrolysis of lignin: Effects of process and upgrading parameters. Bioresour. Technol. 241, 1118–1126.

Feng, J., Jiang, W., Yuan, C., Shi, X., Zang, K., Zhang, Y., 2018. Deposition–precipitation approach for preparing core/shell SiO2@Ni-Rh nanoparticles as an advanced catalyst for the dehydrogenation of 2-methoxycyclohexanol to guaiacol. Appl. Catal. A Gen. 562, 106–113. https://doi.org/10.1016/J.APCATA.2018.06.002

Fermoso, J., Hernando, H., Jiménez-Sánchez, S., Lappas, A.A., Heracleous, E., Pizarro, P., Coronado, J.M., Serrano, D.P., 2017. Bio-oil production by lignocellulose fast-pyrolysis: Isolating and comparing the effects of indigenous versus external catalysts. Fuel Process. Technol. 167, 563–574. https://doi.org/10.1016/j.fuproc.2017.08.009

Giudicianni, P., Gargiulo, V., Grottola, C.M., Alfè, M., Ferreiro, A.I., Mendes, M.A.A., Fagnano, M., Ragucci, R., 2021. Inherent Metal Elements in Biomass Pyrolysis: A Review. Energy & Fuels. https://doi.org/10.1021/acs.energyfuels.0c04046

Hernando, H., Fermoso, J., Moreno, I., Coronado, J.M., Serrano, D.P., Pizarro, P., 2017. Thermochemical valorization of camelina straw waste via fast pyrolysis. Biomass Convers. Biorefinery 7, 277–287. https://doi.org/10.1007/s13399-017-0262-x

Hu, R., Wan, S.Q., Mao, F., Wang, J., 2021. Changes in pyrolysis characteristics of agricultural residues before and after water washing. J. Fuel Chem. Technol. 49, 1239–1249. https://doi.org/10.1016/S1872-5813(21)60073-7

Hu, X., Gholizadeh, M., 2019. Biomass pyrolysis: A review of the process development and challenges from initial researches up to the commercialisation stage. J. Energy Chem.

Huang, C., Zhan, Y., Cheng, J., Wang, J., Meng, X., Zhou, X., Fang, G., Ragauskas, A.J., 2021. Facilitating enzymatic hydrolysis with a novel guaiacol-based deep eutectic solvent pretreatment. Bioresour. Technol. 326, 124696. https://doi.org/10.1016/J.BIORTECH.2021.124696

Huang, M., Ma, Z., Zhou, B., Yang, Y., Chen, D., 2020a. Enhancement of the production of bio-aromatics from renewable lignin by combined approach of torrefaction deoxygenation pretreatment and shape selective catalytic fast pyrolysis using metal modified zeolites. Bioresour. Technol. 301, 122754. https://doi.org/10.1016/j.biortech.2020.122754

Huang, M., Ma, Z., Zhou, B., Yang, Y., Chen, D., 2020b. Enhancement of the production of bio-aromatics from renewable lignin by combined approach of torrefaction deoxygenation pretreatment and shape selective catalytic fast pyrolysis using metal modified zeolites. Bioresour. Technol. 301, 122754. https://doi.org/10.1016/j.biortech.2020.122754

Huang, M., Xu, J., Ma, Z., Yang, Y., Zhou, B., Wu, C., Ye, J., Zhao, C., Liu, X., Chen,

D., Zhang, W., 2021. Bio-BTX production from the shape selective catalytic fast pyrolysis of lignin using different zeolite catalysts: Relevance between the chemical structure and the yield of bio-BTX. Fuel Process. Technol. 216, 106792. https://doi.org/10.1016/J.FUPROC.2021.106792

Jiang, L., Hu, S., Sun, L. shi, Su, S., Xu, K., He, L. mo, Xiang, J., 2013a. Influence of different demineralization treatments on physicochemical structure and thermal degradation of biomass. Bioresour. Technol. 146, 254–260. https://doi.org/10.1016/J.BIORTECH.2013.07.063

Jiang, L., Hu, S., Sun, L., Su, S., Xu, K., He, L., Xiang, J., 2013b. Influence of different demineralization treatments on physicochemical structure and thermal degradation of biomass. Bioresour. Technol. 146, 254–260. https://doi.org/10.1016/J.BIORTECH.2013.07.063

Kabir, G., Hameed, B.H., 2017. Recent progress on catalytic pyrolysis of lignocellulosic biomass to high-grade bio-oil and bio-chemicals. Renew. Sustain. Energy Rev. 70, 945–967. https://doi.org/10.1016/J.RSER.2016.12.001

Khan, S.R., Zeeshan, M., Ahmed, A., Saeed, S., 2021. Comparison of synthetic and low-cost natural zeolite for bio-oil focused pyrolysis of raw and pretreated biomass. J. Clean. Prod. 313, 127760. https://doi.org/10.1016/j.jclepro.2021.127760

Kim, J.S., Lee, Y.Y., Kim, T.H., 2016. A review on alkaline pretreatment technology for bioconversion of lignocellulosic biomass. Bioresour. Technol. 199, 42–48. https://doi.org/10.1016/J.BIORTECH.2015.08.085

Kumar, Avnish, Biswas, B., Saini, K., Kumar, Adarsh, Kumar, J., Krishna, B.B., Bhaskar, T., 2021. Py-GC/MS study of prot lignin with cobalt impregnated titania,

ceria and zirconia catalysts. Renew. Energy 172, 121–129. https://doi.org/10.1016/j.renene.2021.03.011

Kumar, R., Strezov, V., Weldekidan, H., He, J., Singh, S., Kan, T., Dastjerdi, B., 2020. Lignocellulose biomass pyrolysis for bio-oil production: A review of biomass pre-treatment methods for production of drop-in fuels. Renew. Sustain. Energy Rev. 123. https://doi.org/10.1016/j.rser.2020.109763

Leng, E., Wang, Y., Gong, X., Zhang, B., Zhang, Y., Xu, M., 2017. Effect of KCl and CaCl2 loading on the formation of reaction intermediates during cellulose fast pyrolysis. Proc. Combust. Inst. 36, 2263–2270. https://doi.org/10.1016/j.proci.2016.06.167

Li, X., Zhao, Q., Han, M., Zhang, K., Guo, Z., Li, B., Wang, W., Wei, X., Liang, M., 2022. Pyrolysis characteristics and kinetic analysis of tobacco stem pretreated with different solvents. Biomass Convers. Biorefinery. https://doi.org/10.1007/s13399-021-02280-5

Libro del Web de Química del NIST [WWW Document], n.d. URL https://webbook.nist.gov/chemistry/ (accessed 10.17.22).

Liu, C., Duan, X., Chen, Q., Chao, C., Lu, Z., Lai, Q., Megharaj, M., 2019. Investigations on pyrolysis of microalgae Diplosphaera sp. MM1 by TG-FTIR and Py-GC/MS: Products and kinetics. Bioresour. Technol. 294, 122126. https://doi.org/10.1016/J.BIORTECH.2019.122126

M.R., 1981. Infrared characteristic group frequencies : G. Socrates, John Wiley & Sons, Chichester, New York, Brisbane, Toronto, 1980, pp. xi + 153, price £24.00. J. Mol. Struct. 77, 174. https://doi.org/10.1016/0022-2860(81)85280-5

Ma, Z., Ghosh, A., Asthana, N., van Bokhoven, J., 2017. Optimization of the Reaction Conditions for Catalytic Fast Pyrolysis of Pretreated Lignin over Zeolite for the Production of Phenol. ChemCatChem 9, 954–961. https://doi.org/10.1002/cctc.201601674

Mayer, Z.A., Apfelbacher, A., Hornung, A., 2012. A comparative study on the pyrolysis of metal- and ash-enriched wood and the combustion properties of the gained char. J. Anal. Appl. Pyrolysis 96, 196–202. https://doi.org/10.1016/J.JAAP.2012.04.007

Miranda, I., Simões, R., Medeiros, B., Nampoothiri, K.M., Sukumaran, R.K., Rajan, D., Pereira, H., Ferreira-Dias, S., 2019. Valorization of lignocellulosic residues from the olive oil industry by production of lignin, glucose and functional sugars. Bioresour. Technol. 292, 121936. https://doi.org/10.1016/J.BIORTECH.2019.121936

Mlonka-Mędrala, A., Magdziarz, A., Gajek, M., Nowińska, K., Nowak, W., 2020. Alkali metals association in biomass and their impact on ash melting behaviour. Fuel 261, 116421. https://doi.org/10.1016/j.fuel.2019.116421

Mohammed, I.Y., Abakr, Y.A., Kazi, F.K., Yusuf, S., 2017. Effects of Pretreatments of Napier Grass with Deionized Water, Sulfuric Acid and Sodium Hydroxide on Pyrolysis Oil Characteristics. Waste and Biomass Valorization 8, 755–773. https://doi.org/10.1007/s12649-016-9594-1

Niu, Q., Ghysels, S., Wu, N., Rousseau, D.P.L., Pieters, J., Prins, W., Ronsse, F., 2022. Effects of demineralization on the composition of microalgae pyrolysis volatiles in py-GC–MS. Energy Convers. Manag. 251, 114979. https://doi.org/10.1016/j.enconman.2021.114979

Parascanu, M.M., Puig Gamero, M., Sánchez, P., Soreanu, G., Valverde, J.L., Sanchez-

Silva, L., 2018. Life cycle assessment of olive pomace valorisation through pyrolysis. Renew. Energy 122, 589–601. https://doi.org/10.1016/J.RENENE.2018.02.027

Persson, H., Yang, W., 2019. Catalytic pyrolysis of demineralized lignocellulosic biomass. Fuel 252, 200–209. https://doi.org/10.1016/J.FUEL.2019.04.087

Puig-Gamero, M., Alcazar-Ruiz, Á., Sánchez, P., Sanchez-Silva, L., 2020. Binary Blends Versus Ternary Blends in Steam Cogasification by Means of TGA-MS: Reactivity and H<inf>2</inf>/CO Ratio. Ind. Eng. Chem. Res. 59. https://doi.org/10.1021/acs.iecr.0c01399

Puig-Gamero, M., Parascanu, M.M., Sánchez, P., Sanchez-Silva, L., 2021. Olive pomace versus natural gas for methanol production: a life cycle assessment. Environ. Sci. Pollut. Res. https://doi.org/10.1007/s11356-021-12710-6

Schmidt, R.J., 2005. Industrial catalytic processes - Phenol production. Appl. Catal. A Gen. 280, 89–103. https://doi.org/10.1016/j.apcata.2004.08.030

TAPPI, 2018. TAPPI/ANSI Test Method T 401 om-15 - Fiber analysis of paper and paperboard.

Torres, D., Pérez-Rodríguez, S., Cesari, L., Castel, C., Favre, E., Fierro, V., Celzard, A., 2021. Review on the preparation of carbon membranes derived from phenolic resins for gas separation: From petrochemical precursors to bioresources. Carbon N. Y. 183, 12–33. https://doi.org/10.1016/J.CARBON.2021.06.087

Volpe, M., D'Anna, C., Messineo, S., Volpe, R., Messineo, A., 2014. Sustainable production of bio-combustibles from pyrolysis of agro-industrial wastes. Sustainability 6, 7866–7882.

Wang, H., Srinivasan, R., Yu, F., Steele, P., Li, Q., Mitchell, B., 2011. Effect of acid, alkali, and steam explosion pretreatments on characteristics of bio-oil produced from pinewood. Energy and Fuels 25, 3758–3764. https://doi.org/10.1021/ef2004909

Wang, S., Dai, G., Yang, H., Luo, Z., 2017. Lignocellulosic biomass pyrolysis mechanism: A state-of-the-art review. Prog. Energy Combust. Sci. 62, 33–86. https://doi.org/10.1016/J.PECS.2017.05.004

Xu, J., Zhang, Y., Shen, Y., Li, C., Wang, Y., Ma, Z., Sun, W., 2019. New perspective on wood thermal modification: Relevance between the evolution of chemical structure and physical-mechanical properties, and online analysis of release of VOCs. Polymers (Basel). 11. https://doi.org/10.3390/polym11071145

Zhang, Y., Lei, H., Yang, Z., Qian, K., Villota, E., 2018. Renewable High-Purity Mono-Phenol Production from Catalytic Microwave-Induced Pyrolysis of Cellulose over Biomass-Derived Activated Carbon Catalyst. ACS Sustain. Chem. Eng. 6, 5349–5357. https://doi.org/10.1021/acssuschemeng.8b00129

Zhang, Y., Lv, P., Wang, J., Wei, J., Cao, P., Bie, N., Bai, Y., Yu, G., 2022. Product characteristics of rice straw pyrolysis at different temperature: Role of inherent alkali and alkaline earth metals with different occurrence forms. J. Energy Inst. 101, 201–208. https://doi.org/10.1016/j.joei.2022.01.016